POLITECNICO DI TORINO
Repository ISTITUZIONALE

AI technology for remote clinical assessment and monitoring

Original
AI technology for remote clinical assessment and monitoring / Zoppo, G., Marrone, F., Pittarello, M., Farina, M., Uberti, A., Demarchi, D., Secco, J., Corinto, F., Ricci, E.. - In: JOURNAL OF WOUND CARE. - ISSN 0969-0700. - STAMPA. - 29:12(2020), pp. 692-706. [10.12968/jowc.2020.29.12.692]

Availability:
This version is available at: 11583/2858162 since: 2020-12-21T11:41:54Z

Publisher:
MA Healthcare Ltd

Published
DOI:10.12968/jowc.2020.29.12.692

Terms of use:

This article is made available under terms and conditions as specified in the corresponding bibliographic description in the repository

Publisher copyright

(Article begins on next page)

27 November 2026

AI technology for remote clinical assessment and monitoring

Objective: To report the clinical validation of an innovative, artificial intelligence (AI)-powered, portable and non-invasive medical device called Wound Viewer. The AI medical device uses dedicated sensors and AI algorithms to remotely collect objective and precise clinical data, including three-dimensional (3D) wound measurements, tissue composition and wound classification through the internationally recognised Wound Bed Preparation (WBP) protocol; this data can then be shared through a secure General Data Protection Regulation (GDPR)- and Health Insurance Portability and Accountability Act (HIPAA)-compliant data transfer system. This trial aims to test the reliability and precision of the AI medical device and its ability to aid health professionals in clinically evaluating wounds as efficiently remotely as at the bedside.

Method: This non-randomised comparative clinical trial was conducted in the Clinica San Luca (Turin, Italy). Patients were divided into three groups: (i) patients with venous and arterial ulcers in the lower limbs; (ii) patients with diabetes and presenting with diabetic foot syndrome; and (iii) patients with pressure ulcers. Each wound was evaluated for area, depth, volume and WBP wound classification. Each patient was examined once and the results, analysed by the AI medical device, were compared against data obtained following visual evaluation by the physician and research team. The area and depth were compared with a Kruskal–Wallis one-way analysis of variations in the obtained distribution (expected p-value>0.1 for both tests). The WBP classification and tissue segmentation were analysed by directly comparing the classification obtained by the AI medical device against that of the testing physician.

Results: A total of 150 patients took part in the trial. The results demonstrated that the AI medical device's AI algorithm could acquire objective clinical parameters in a completely automated manner. The AI medical device reached 97% accuracy against the WBP classification and tissue segmentation analysis compared with that performed in person by the physician. Moreover, data regarding the measurements of the wounds, as analysed through the Kruskal–Wallis technique, showed that the data distribution proved comparable with the other methods of measurement previously clinically validated in the literature (p=0.9).

Conclusion: These findings indicate that remote wound assessment undertaken by physicians is as effective through the AI medical device as bedside examination, and that the device was able to assess wounds and provide a precise WBP wound classification. Furthermore, there was no need for manual data entry, thereby reducing the risk of human error while preserving high-quality clinical diagnostic data.

Declaration of interest: The project was funded by a Proof of Concept grant from Politecnico di Torino and the Start Cup grant from I3P and Regione Piemonte. The authors have no conflicts of interest.

automatic wound classification • medical device • telemedicine • three-dimensional wound measurement • wound bed preparation score • wound care • wound healing • wound measurement techniques • wounds

Skin ulcers are a chronic pathological condition affecting around 1–2% of the world's population.[1] In Europe alone, over four million patients are affected by this syndrome, costing €4 billion in national health treatment every year.[1] Primarily found in people >65 years of age (>60%), skin ulcers are commonly associated with pre-existing chronic diseases such as diabetes, vascular problems, heart disease and obesity.[2] Early detection and assessment of the wound is vital; after four weeks there is a 30% chance of the lesion never healing, a 50% chance of loss of limb and a 50% chance of mortality in the following five years.[3]

Chronic pain, reduced mobility, and psychological and emotional stress are just a few of the difficulties commonly experienced by patients with this skin condition.[4] Furthermore, treatment of skin ulcers may prove lengthy, taking several months or even years for the wound to heal.[4] In many patients, complications arise that require urgent surgical intervention leading to long periods of hospitalisation.[5]

Until recently, hospitalisation and inpatient assistance were considered the safest and most effective means to providing wound treatment and to ensuring continuous monitoring; this, however, is costly, and so there has been a move toward home care assistance.[4,5] This has led to the preference for a telemedical approach involving remote monitoring—more suitable both from an economic and patient experience point of view. However, prompt intervention can prove difficult, and health professionals must be able to ensure a high standard of care. Patients treated in home care assistance facilities fall under the responsibility of numerous health professionals, making it vital that all clinical information is shared in a precise and standardised way.

Gianluca Zoppo,[1] PhD Candidate; **Francesco Marrone**,[1] PhD Candidate; **Monica Pittarello**,[2] Research Nurse; **Marco Farina,**[1] Research Fellow; **Alberto Uberti,**[3] Research Fellow; **Danilo Demarchi,**[1] Associate Professor; **Jacopo Secco,**[1] Research Fellow*; **Fernando Corinto,**[1] Full Professor; **Elia Ricci,**[1] Head of Department
***Corresponding author email:** jacopo.secco@polito.it
1 Department of Electronic Engineering and Telecommunications, Politecnico di Torino, Corso Duca degli Abruzzi 24, 10129, Torino, Italy. **2** Department of Surgery 2, Clinica San Luca, Strada della Vetta 3, 10020, Torino, Italy. **3** Department of Management Engineering, Politecnico di Torino, Corso Duca degli Abruzzi 24, 10129, Torino, Italy.

© 2020 MA Healthcare ltd

Downloaded from magonlinelibrary.com by 130.192.232.213 on December 16, 2020.

As yet, there are few technological support tools for wound care professionals that have provided reliable morphological ulcer measurement, and none are able to provide automatic diagnostic information through a standardised wound classification scale.[6,7]

Such a constant, standardised monitoring protocol for sharing patient information would also allow health professionals to act more quickly. In a study by Pillon, it was demonstrated how telemedical methods would not only lower the costs of wound care treatment (by 35%), but they would also increase the wound healing rate (90% instead of 75%) and patients' quality of life.[8] According to this study, due to the use of digital patient records and integrated data sharing, none of the 175 patients studied required hospitalisation.[8]

Smith-Strøm et al. studied telemedical monitoring in the treatment of diabetic foot ulcers (DFUs) and showed it to be a relevant alternative to inpatient treatment,if there is the means to ensure precise, efficient and secure clinical data.[9] Bolton demonstrated the cost-effectiveness and positive outcomes of a systematic telemedical approach to wound management for various types of hard-to-heal wounds, ranging from pressure ulcers (PUs) to venous and arterial ulcers.[10]

Wound Viewer (Omnidermal, Italy), an artificial intelligence (AI)-powered medical device, was developed based on the above clinical requirements as an easy-to-use, fast and precise tool that also permits the secure exchange of validated clinical data on patients between health professionals. It was designed for use by all clinical operators, ranging from the less specialised to the most expert in wound management. Its features, which include an autocalibration of its distance sensors and an automatic analysis of the wound bed for wound bed preparation (WBP) protocol classification,[11] render the device capable of performing precise assessments independently from the operator.

The device was developed following an in-depth study undertaken in collaboration with physicians and professionals with extensive experience in the treatment and management of wounds. All data collected by the system have been validated in order to deliver full analysis of the lesion and the patient, even if used by less-experienced operators, and to share the clinical information with specialised physicians so they can ensure a standard of treatment on a par with bedside monitoring, even in a telemedical set-up.

Clinical overview

Quantification in wound care is a grey area in which many works have been published but authors have yet to reach a consensus. A number of parameters are measured. The work of Mani et al. remains one of the cornerstones, listing the various measurement possibilities.[12] The pH is intended to be an indicator of tissue repair, considering also its role in the microenvironment of the wound bed.[13] Transcutaneous oxygen and flow at the microcirculatory level are important, but only as indicators of possible results in terms of tissue vitality.[12] The fact that a skin ulcer has a defined area and volume, although not simply measured, has led many authors to further investigation. For clinicians, the objective of measuring is to be able to better define the evolution of a wound, whether it is being repaired, blocked or worsened; Flanagan et al. define wound reduction parameters as repair indicators.[14] Sheehan et al. have demonstrated that, in the case of diabetic ulcers, early assessment (within four weeks) is crucial for full recovery.[15] Gorin et al. have analysed the reduction of wound area, width and length, and concluded that a linear parameter is independent of the geometric shape of the wound.[16] Cukjati et al. reiterate how wound area and its variations indicate evolution and prognostics.[17] Moreover, the percentage change of the wound area is a clinically recognised prognostic measure, although the problem remains of how to measure it.[6,7]

Wound area is not the only prognostic indicator. We propose that a subdivision of the lesions—in terms of tissue type and exudate management—may be considered an appropriate indicator of clinical results. We have used the WBP score proposed by Falanga as an analysis parameter as it is well known and used on different types of wounds.[11] Table 1 describes the WBP score as proposed by Falanga.

Prompt, accurate wound assessment using the WBP score is essential in clinical practice, as it is one of the parameters to be considered in choosing the most appropriate and effective treatment.[18] A correct WBP scoring for wounds presenting eschar, and thus necrotic tissue, which Table 1 lists as class D, encounters a number of problems in normal clinical practice as shown by Tong.[19,20] It has been demonstrated, for example, that any miscalculation of a lesion and therefore incorrect treatment within the first four weeks would, in 30% of cases, mean that wound not healing; in 50% of cases, patients would require surgical amputation of the limb, and there would be a 50% chance of death in the following five years.[15] The most common problem wound care clinicians encounter is that of correctly identifying wounds about to enter the necrotic phase.[21] This may be for a variety of reasons, such as the presence of a small amount of necrosis compared with the dimension of the entire wound bed. Moreover, eschar can present itself in different

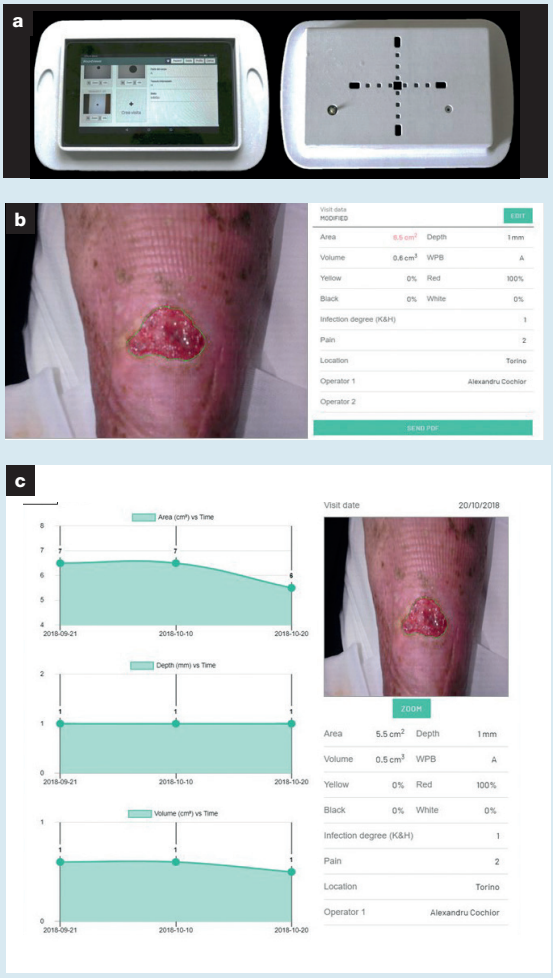
Table 1. Description of the Wound Bed Preparation score as presented by Falanga[11]

Wound bed appearance					Wound exudate
Score	Granulation	Fibrinous	Eschar	Score	Description
A	100%	–	–	1	Fully controlled
B	50–100%	+	–	2	Partially controlled
C	<50%	+	–	3	Uncontrolled
D	Any	+	+		

© 2020 MA Healthcare ltd

Downloaded from magonlinelibrary.com by 130.192.232.213 on December 16, 2020.

Fig 1. Wound Viewer: on one side the capacitive touch screen is displayed with the user interface, while the other shows the digital camera, the 16 infrared sensor-array and the four white light-emitting diodes (**a**). An example of the user interface showing the result of an examination (**b**). An example of the wound statistics page, designed for health professionals to monitor the wound's evolution (**c**)



compositions, both morphological and molecular, as described by Thomas et al.[21] Although several treatments are available for wound debridement, for example that proposed by Durham et al.,[22] and the composition of debridement is well known,[23] there are still few, if any, ways to identify and monitor this kind of tissue in a standardised and accurate way.

The AI medical device algorithm has been refined on more than 500 hard-to-heal wound cases, with patients of different ethnicities and so with different skin tones. The device is able to perform morphological wound measurements automatically, segmenting the wound bed composition and ranking the lesion through its WBP score. It is connected to a secure data transfer system that instantly updates all health professionals involved in treating the patient.

Introduction to the AI medical device

A customised AI medical device, it has been developed to run the proprietary AI algorithm for wound measurement and assessment. The device, shown as a prototype in Fig 1a, is equipped with a custom-designed electronic board mounting a five-megapixel colour complementary metal oxide semiconductor (CMOS) camera sensor for high resolution pictures, 16 high precision infrared (IR) distance sensors and four white light-emitting diodes (LED)s.[24] The LEDs are placed at a distance of 5cm from the CMOS camera eliminating shadows from any photographs taken by the device. Moreover, these light sources are set to a standard intensity, ensuring uniformly lit pictures which can be analysed against a standard colour scheme. Operators control the device through a special front end via a capacitive touch screen display. Typical use of the device in the field is represented thus:

- Point the device towards the wound, keeping it parallel to the surface
- The 16 IR distance sensors calibrate the focal ratio of the camera
- Select the region of interest (ROI) of the wound by drawing a rough rectangle on the image on the screen
- The picture is analysed by the algorithm
- All relevant information computed is shown on the display (wound area, depth, tissue segmentation and WBP score classification).

In addition to taking high precision measurements of the patient's wound, the device stores all data in a secure and General Data Protection Regulation (GDPR)-compliant digital database, allowing the wound to be monitored as it evolves. This monitoring scheme, shown in Fig 1b and 1c, permits physicians to immediately verify how effective the chosen therapy is through a quantitative series of indicators.

The AI medical device algorithm applies discrete time-cellular nonlinear network (DT-CNN) computing architecture to identify the wound and provide relevant measurements.[25–28] The clinical data acquired include wound area expressed in cm^2, wound depth expressed in mm and wound granulation through the WBP score.[11] DT-CNN is a parallel computing paradigm, introduced by Chua and Yang, similar to artificial neural networks for processing signals of any dimension.[29,30]

As with any other bioinspired neuromorphic algorithm, the DT-CNN passes through a learning and an inference phase. In the learning phase, the cellular nonlinear network in the Wound Viewer algorithm, which processes a two-dimensional colour image, is provided with statistical information about the tissue forming the wound bed through colour analysis. Those statistics are extrapolated from the trial group by digitally segmenting wound areas in the images contained in the trial group (more than 500 wound pictures). The resulting statistical information takes the form of mapping between each of the 16,777,216 (4096^2) possible 24-bit red/green/blue (RGB) colours and the number of times that one colour occurs in the wound areas contained in the trial group.

© 2020 MA Healthcare ltd

Downloaded from magonlinelibrary.com by 130.192.232.213 on December 16, 2020.

The nonlinear processing units making up DT-CNNs are often referred to as neurons or cells.[31] Depending on the underlying technology, these cells may be implemented as arbitrary units computing independently, resulting in an extremely rapid parallel algorithm. For example, the elaboration results of the wounds in Fig 2a are reported in Fig 2b. The original images in Fig 2a were subjected to a preprocessing phase before being presented to the trained DT-CNN. Each automated part of the network used the statistical chromatic knowledge stored in the device. The output of the analysis was then computed by counting the number of pixels in a given proximity whose colour appeared often enough in the wounds from the trial group. The total number of pixels confirmed to be characteristic of a wound area is then compared against a threshold. If this critical value is lower than the weighted number of pixels accounted for then the pixel is reported to be part of a wound area (set to binary true); otherwise it is rejected (set to binary false). Finally, the binary mask is newly processed to find the borders and then overlapped onto the original image (shown in Fig 2b). The borders of the mask are shown in green.

The 16 IR sensors measure distances concurrently as the CMOS camera takes the digital photographs. These distance measurements are fundamental in calculating the depth and area of the patient's wound. Given the cross disposition of the 16 IR sensors, wound depth is calculated as the difference between the distance reading given by the outermost sensors and that given by the central sensors. Wound area, on the other hand, relies solely on the average reading given by the outermost sensors. This distance measurement is converted into a coefficient through a calibration mapping uploaded onto the tablet during manufacture.

Regarding wound classification, the algorithm only takes into account those pixels that were recognised as part of the wound (i.e., the elements that reside within the green contour in Fig 2b). Once the entire surface of the wound has been recognised, the highlighted elements are analysed by colour scheme (RGB). All possible pixel colour sets forming the wound were classified into four macro groups: red, white, black and yellow. The wound images in the trial group were ranked using WBP score and the algorithm then matched the colour schemes read within the area of the image depicting the wound. The algorithm uses this test phase to analyse these colour schemes and automatically classify them.

The AI medical device was also designed to facilitate secure data exchange among health professionals. The device and its software have been integrated with the Amazon Web Service (AWS) cloud system. Where necessary, all data collected in a single device can be stored in a secure, private cloud database and sent automatically to all other devices held by those professionals who have access to a specific patient's records. The database and transmission protocols were designed and implemented to be compliant with all current data regulations (GDPR for the European Union and Health Insurance Portability and Accountability Act (HIPPA) for the US). This function allows all physicians and clinical operators using the system to be immediately updated on the status of their entire patient base while guaranteeing a high standard of care.

Methods

Brief description of other wound assessment methods used in the trial

The results obtained using the AI medical device were compared with the results given by three other wound analysis and measurement methods. The devices used in the study were:

- VISITRAK (Smith+Nephew, US) is a wound measurement active board formerly distributed by Smith and Nephew. The device, shown in Fig 3b, comes with a tracing pen and a set of scaled transparent acetate sheets. During examination, the operator places one of the scaled acetate sheets on the injured limb, entirely covering the wound and, using a non-toxic marker, traces the wound contours on the transparent sheet, which is then placed on the active board. Using the special pen provided, the contour is again traced so the board can identify the edges of the lesion. When the board senses that a closed surface has been drawn, the device calculates the wound's surface. No other parameters regarding depth or tissue segmentation are calculated
- MOWA (Health Path, Italy) is an app for Apple IOS mobile platforms. It is not associated with a specific physical device, using the camera of the mobile device on which the app is installed to take photographs and its touch screen to control the functions. The initial interface of the app is shown in Fig 3c. Firstly, the operator places a small paper token showing a blue circle of known, constant dimensions near to the wound. Then, the camera is activated and the wound is photographed, ensuring that the token

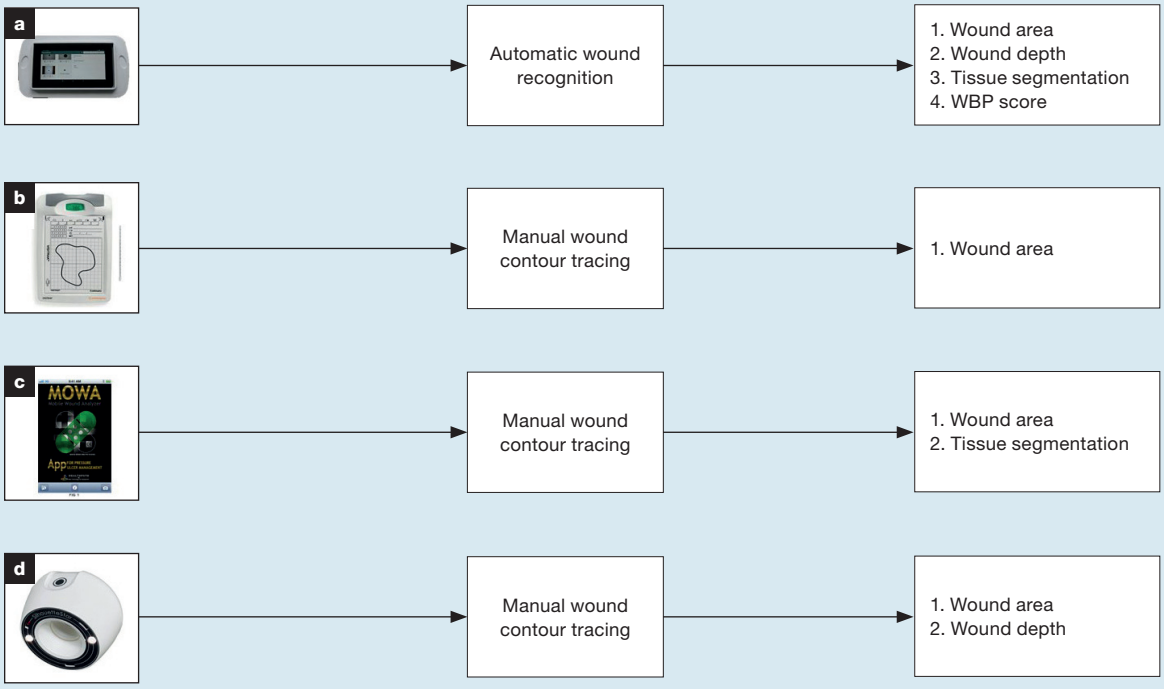
Fig 2. Original images of venous and arterial lower limb ulcers from three different patients taken with the AI medical device during the trial (**a**). Representation of the result of the AI medical device cellular automaton identifying the wound's edges (in green) (**b**). The edges of the wound coincide with the borders of the binary mask given by the discrete time-cellular nonlinear network (DT-CNN)



© 2020 MA Healthcare ltd

Downloaded from magonlinelibrary.com by 130.192.232.213 on December 16, 2020.

Fig 3. Devices, procedures and results obtained with the different systems used in the trial: Wound Viewer (**a**); VISITRAK (**b**); MOWA (**c**); Silhouette (**d**). The parameters calculated by each system are listed on the right for each device. WBP—wound bed preparation



is entirely visible in the picture. This image is displayed on the screen of the device on which the operator then manually segments the edges of the wound. Subsequently the device calculates the surface of the wound and automatically segments the tissues composing the wound bed into granular, fibrin and necrotic

- Aranz Silhouette (Aranz Medical, New Zealand) system is composed of the Star (Fig 3d), an image acquisition tool comprising three laser arrays, a digital camera and two LEDs for image light control. The three laser arrays each project a beam of light which intersect in a star-shaped form when the device is at the proper distance to correctly acquire the picture. The lasers have to intercept at the centre of the wound and the system uses the beams to calculate the depth of the wound. The system has to be connected to a computer, which has to be equipped with the specific image analysis software provided by Aranz, through a USB cable. Once the image is taken, it is sent to the connected computer and displayed to the operator. The operator then manually traces the contours of the wound on the image using the mouse or track pad. Once this is done, the system provides the surface and depth measurements of the wound. The operator has to manually insert all other parameters on the specific software installed on the computer and then saves the information.

As shown in Fig 3, all devices used in comparison with the AI medical device require manual segmentation of wound edges. This procedure may prove invasive for the patient. The AI medical device, on the other hand, does not require any invasive manual intervention, thanks to its trained AI algorithm. It is able to automatically recognise the wound merely by analysing the image taken, and then return all the parameters listed on the right-hand side (Fig 3a), including area, depth, tissue segmentation and wound classification against the WBP score.

Study rationale

Skin ulcers are treated with continuous and periodic dressings by the specialist in charge. During a normal medication session, the health professional removes the previous bandage, visually assesses the extent of the wound and, depending on the circumstances, applies a fresh dressing. Wound evaluation requires consideration of three essential parameters and how they vary over time (compared with previous examinations). The main characteristics that distinguish whether a wound is healing or worsening are surface extension, depth and colour (representing tissue composition). The devices currently on the market are more time-consuming and less intuitive because there is no automatic wound detection and therefore the intervention of an operator is always required. The purpose of this clinical trial was therefore to verify the capability of operators in correctly acquiring accurate ulcer data with the AI medical device

© 2020 MA Healthcare ltd

Downloaded from magonlinelibrary.com by 130.192.232.213 on December 16, 2020.

in comparison with the other technologies available on the market. Wound bed evaluation is the most important clinical parameter, used both as an indicator of how the implemented treatment evolves and as a guide for therapeutic decisions. The current situation is mainly determined by the experience of the operators, which is subjective and difficult to standardise. The AI medical device's technology aims to overcome the subjectivity inherent in the system by standardising evaluation.

Specifically, the trial aimed to verify the AI medical device's ability to identify skin ulcers on a patient, acquire the image and simultaneously provide data on it (surface extension, depth and colouring), while testing the reliability percentage and margin of error, both on individual data acquisitions and statistically relevant samples.

Ethical approval

The clinical trial, design and the endpoints described below were validated by the Ethical Committee of the Azienda Opedaliero Universitaria San Luigi Gonzaga (Orbassano, Italy) on 3 October 2017 (protocol number OC15194).

To be admitted to the study, all patients had to sign a written informed consent which was also validated by the Ethical Committee of the Azienda Opedaliero Universitaria San Luigi Gonzaga. The document presented to and signed by the patients included their explicit consent to the use of their data by the trial promoters, as well as all photographic images taken for the scientific validation of the AI medical device technology and for eventual scientific publications. Therefore, all individuals whose photographs and data are reported in this manuscript have given prior written informed consent to publish these case details.

Study design and protocol

The trial was conducted in Clinica San Luca (Torino, Italy) as a prospective observational, comparative, non-randomised and monocentric study. The study entailed the acquisition and comparison of photographic images of dermal ulcers using three different methods: Wound Viewer and the three different systems currently used for dermatological wound care. The type of study was not randomised because the same lesions were used to compare the evaluation of the parameters detected instrumentally by operators.

The study looked at 150 patients, divided into three groups based on their aetiology:

- Lower limb ulcers: 50 lesions
- Diabetic foot ulcers: 50 lesions
- Pressure ulcers: 50 lesions.

Table 2 lists the inclusion and exclusion criteria for patient admission.

This analysis aimed to test the function and efficiency of the device for the acquisition of skin ulcer images, in terms of area, depth, volume and colour scale, and compare it with three other validated products currently on the market, and listed in the Methods section. The parameters measured and compared were: ulcer extension (cm^2), ulcer depth (mm) and colorimetric scale (WBP score). Table 3 lists the primary and secondary endpoints of the study.

The devices and methods listed used for comparison were used as 'imperfect control' marks—their measurements were used as a reference point by taking into account the error index declared by their respective manufacturers. From the operative point of view, each lesion was assessed simultaneously through clinical judgment and the different systems available. Only one examination was planned and no check-ups were organised over time. The various image acquisition systems acquired the parameters of each wound, as shown in Table 4.

The study was undertaken by two separate teams: a clinical assessment team comprising two physicians and one registered research nurse at the Clinica San

Table 2. Inclusion and exclusion criteria for patient admission

Inclusion criteria	Exclusion criteria
Chronic skin damage	Acute skin damage
Absence of undermining	Presence of undermining
Informed consent	Failure to obtain informed consent
Wounds >2cm^2	Wounds <2cm^2
Wounds <100cm^2	Wounds >100cm^2

Table 3. Primary and secondary endpoints of the study

Primary endpoints	Secondary endpoints
Evaluation of the detection of the area with the different systems. The evaluation is performed through the data provided by the various validated devices on the market	Definition of wound bed colorimetry and granulation through wound bed preparation score
	Depth assessment
	Analysis regarding the data acquisition time

Table 4. Evaluation methods of the various parameters measured in the study

Parameter	Evaluation method
WBP Score	1. MOWA 2. Wound Viewer 3. Visual clinical evaluation
Area	1. Silhouette 2. MOWA 3. VISITRAK 4. Wound Viewer
Depth	1. Silhouette 2. Wound Viewer 3. With a scaled probe

WBP—wound bed preparation

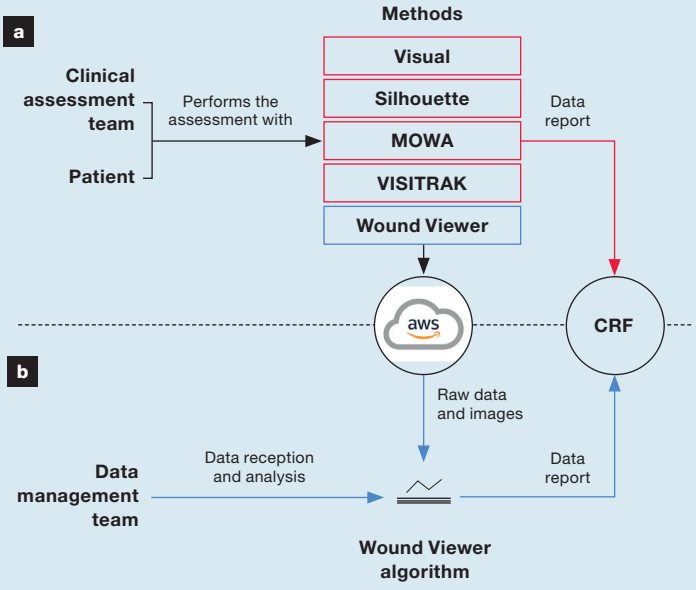
© 2020 MA Healthcare ltd

Downloaded from magonlinelibrary.com by 130.192.232.213 on December 16, 2020.

Luca and a data management team comprising two data managers and a technician at the Politecnico di Torino. Each patient was enrolled by the clinical assessment team which was responsible for verifying the inclusion criteria of the subjects and collecting the consent forms. After enrolment, the wounds were assessed the same day at the Clinica San Luca surgical ward, both visually and using the devices according to the parameters listed in Table 4. In addition, the clinical assessment team was responsible for compiling the clinical research folders (CRF) with the data collected through all wound assessment methods used, except Wound Viewer. During the trial, the AI medical device was programmed to simply collect the raw data needed to allow its algorithm to perform the required analyses and transfer it to the data management team through the AWS cloud system. The onboard wound assessment algorithm was deactivated on the AI medical device and run by the data management team at a later time for a double-blind comparison of the wound assessments and to test the data transfer functionality of the system. Having received the raw data and images from the AI medical device, the data management team used the proprietary AI algorithm to perform the analyses and compile the corresponding CRFs. A technician participating in the study was responsible for solving any technical problems arising in the devices. A detailed workflow of the patient and data management is shown in Fig 4.

After officially enrolling the patients, the clinical assessment team assessed the wound using all the technological and clinical methods involved in the study. Unlike the other devices, the AI medical device was programmed to simply collect the raw images and data necessary to run the proprietary wound assessment AI algorithm and transfer it through AWS to the data management team (Fig 4, blue flow lines). The latter then ran the algorithm with the received data and reported the results on the CRF. The data collected through all other technologies and methods were directly reported on the CRF by the clinical assessment team (Fig 4, red flow line).

Fig 4. Workflow of the clinical trial performed at San Luca (**a**) and the Politecnico di Torino (**b**). CRF—clinical research folders



Statistical analysis

The data returned by the AI medical device and the control devices were compared by formulating a distribution curve set against an equivalent curve (comparable to the Weibull distribution regarding area measurements and a Gaussian distribution regarding depth measurements). The mean value and variance of the obtained curve was used to generate an appropriate fitting distribution curve. Statistical goodness-of-fit was assessed by comparing the obtained curves and distribution. The Kruskal–Wallis test had an acceptance condition (H0 is the hypotheses on whether or not the distributions can be considered statistically comparable) set to a p-value of ≥0.1. This non-parametric test substitutes the one-way analysis of variance (ANOVA) test in the case of non-normal populations.

The colorimetric index was evaluated using the WBP scale. The devices' WBP scores were compared with those obtained by physicians during clinical visual assessment. This kind of analysis aims to establish the sensitivity of the device and compare it with the relative sensitivity of other already validated systems.

Results

Wound classification for remote precision monitoring

The first analysis undertaken compared the ability to identify the tissues composing the wound bed and the WBP score classification of the wound. This analysis was intended to verify the ability to correlate the colour segmentation of the wound bed against the correct WBP score and to compare its result with the one given by the clinical assessment team who examined the patient in person. To avoid reciprocal influence between the two classifications, the clinical assessment team was not privy to the results delivered by the algorithm. The raw images were sent automatically to the AWS platform and gathered by the data management team (Fig 4), who ran the AI medical device algorithm on the wound images and gathered the information in a double-blind fashion. The protocol was designed not only to verify the classification accuracy of the device, but also to prove that the AI medical device allows trained physicians to gather precise, reliable clinical information in a telemedical configuration, as if they were performing the same examination directly on the patient.

Fig 5 shows how the WBP classifications undertaken by the AI medical device (Fig 5a) and MOWA (Fig 5b) compare with those undertaken by the clinical assessment team through visual analysis. The heat points that reside on the diagonal of each graph (from top left side to bottom right side) reveal the number of

© 2020 MA Healthcare ltd

Downloaded from magonlinelibrary.com by 130.192.232.213 on December 16, 2020.

cases in which the classifications matched. On the other hand, the heat points outside the diagonal count the cases where there was a mismatch in the wound classification. Fig 5a illustrates the confusion matrix's heat map between the AI medical device's classifications and the clinical assessment performed by the physician. From the heat map results, we found that most of the inferred classes perfectly match the physician's visual assessment, with an accuracy of 0.97 overall. Fig 5b illustrates the confusion matrix's heat map between MOWA classifications and the clinical assessment performed by the physician. Clearly, the matrix shows a different pattern, with a larger occurrence of misclassification (accuracy of 0.53 overall) and some additional cases that were not recognised by the device (N/D class).

The WBP wound classification performed by the AI medical device consists of analysing the tissue composing the wound through a combination of four macro-groups of colours: red, yellow, white and black. As an example, Fig 6 describes four cases that were assessed during the trial, one for each WBP class. The first (Fig 6a) consists of a wound which is completely composed of granular tissue, classified as A. In the second (Fig 6b) the presence of slough can be noted (<50%), classified as 'B'. Fig 6c shows a wound with <50% slough, and in Fig 6d the wound depicted presents with necrosis. The last column of the picture reports the result of the colour analysis returned by the Wound Viewer algorithm.

As seen by the results in Fig 5, by the end of the trial around 50 wounds were classified as 'D' (according to the WBP scale), meaning that these wounds presented necrotic tissue, even at a low percentage. 'D' classified wounds require more attention by health professionals because of their highly advanced state of deterioration. The results of the analysis showed that the AI medical device was able to recognise these particular wounds with high precision, proving at first that the objective for which the device was designed was reached. Fig 7 shows three examples of wounds examined in the trial to better demonstrate the correct tissue classification capabilities of the AI medical device. As in the rest of the cases, all three wounds were classified as 'D' according to the WBP score, both by the examining physician (unaware of the AI medical device analysis) and by the AI medical device, which was able to send accurate raw data and images of the lesions to the data management team through the AWS cloud system. According to Shultz et al., a wound is classified as 'D' when it presents eschar (necrosis), fibrinous tissue and any amount of granular tissue.[11,32] The images shown in Fig 7 range from a very low amount of necrotic tissue detected by the AI medical device (7.3% in Fig 7a), to a very large amount (96.4% in Fig 7c).

Morphological measurement precision

This analysis evaluated the assessment of the wound's area measurement by comparing the data obtained from the AI medical device with the corresponding measurements collected by three other wound analysis and measurement methods. An initial descriptive analysis is shown in the box plots of Fig 8 where most of the data for all four detectors ranges between 3cm^2 and 15cm^2. However, although outliers are clearly present, the box plots illustrate similar distributions of the data collected by the four devices.

This is also reflected in the histograms of Fig 9, which portray a high degree of similarity in shape and scale: most occurrences are very close to the origin, whereas the remainder rapidly decrease toward zero.

Since such behaviour is typical in Weibull distributions, shape and scale parameters were estimated and subsequently used in a Kolmogorov–Smirnov test to confirm that the four populations were dispersed according to these Weibull distributions. Table 5 shows the estimated parameters and the corresponding values. As is shown, the values are almost identical and therefore, in order to support the hypothesised similarity of distributions, a Kruskal–Wallis one-way ANOVA was performed. The test resulted in a p-value of 0.9, affirming that the hypothesis by which the distributions portray the characteristics of the same population is correct.

Fig 5. Heat map showing how the wound bed preparation (WBP) score wound classification obtained with Wound Viewer compares with those obtained through visual clinical analysis (**a**). Heat map showing how the WBP score wound classification obtained with MOWA compared with those obtained through visual clinical analysis (**b**). The wound assessment performed in a completely automated fashion with Wound Viewer concurred with the classification made through visual analysis by a physician in 96% of cases. On the other hand, almost half of the assessments made with MOWA disagreed with those made by the physician (53% accuracy) and in some cases the system was not able to classify the wound at all. A—only granular tissue; B—<50% slough; C—>50% slough; D—necrosis present; N/D—not determined

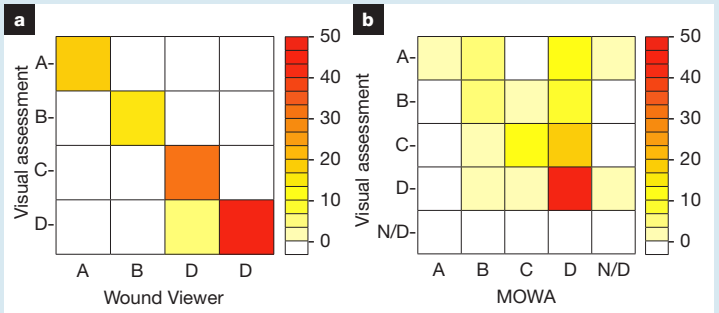


Table 5. Shape and scale parameters of the overlapping Weibull distributions of the area measurements and the p-value calculated through the Kruskal–Wallis one-way analysis of variance test

	Wound Viewer	Silhouette	MOWA	VISITRAK
Shape	0.9475	0.9444	0.9032	0.9316
Scale	10.2809	9.9032	10.1946	10.4722
P-value (Ks-test)	0.4361	0.6179	0.6405	0.4200

© 2020 MA Healthcare ltd

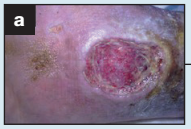
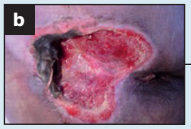
Downloaded from magonlinelibrary.com by 130.192.232.213 on December 16, 2020.

Fig 6. Four examples of wounds assessed during the trial. The first column shows the classification for each wound made by the clinical assessment team through visual analysis. The second column shows the automatic classification performed by the AI medical device algorithm. The third shows the clinical characteristics that led to their classification, as in Falanga et al.[11] The fourth shows the result of the colour analysis performed by the AI medical device algorithm. WBP-wound bed preparation

	Physician's blind evaluation (WBP)	AI medical device evaluation (WBP)	Clinical characteristics	AI medical device colour analysis
 a	A	A	Completely composed of granular tissue	100% Red 0% Yellow 0% White 0% Black
 b	B	B	<50% of slough, no necrosis	82% Red 11% Yellow 7% White 0% Black
 c	C	C	>50% of slough, no necrosis	45% Red 32% Yellow 23% White 0% Black
 d	D	D	Presence of necrosis	23% Red 36% Yellow 3% White 38% Black

The scatter plot in Fig 10a shows the AI medical devices's measurements on the x-axis and the measurements of all the other devices on the y-axis. The data is distributed along the diagonal, indicating a remarkable consistency between the corresponding measures. However, analysing the residuals (Fig 10b–d) of the linear models, it is interesting to note how Wound Viewer, Silhouette and VISITRAK have smaller mean relative errors of 14%, whereas MOWA seems to be less reliable, with mean relative errors of 23%. These errors were computed by considering the three other wound analysis and measurement methods as imperfect controls; however, it should be noted that for large areas, MOWA's precision appears to be remarkably lower, with some deviations that differ from the other devices' measurements by 30%.

Fig 7. Three examples of wounds analysed during the trial. All three wounds were classified both by the physician and by the AI medical devicer as D (presenting eschar or necrotic tissue) at different percentages (as detected by the device): 7.3% (**a**), 37.6% (**b**) and 96.4% (**c**)

	Physician's blind evaluation (WBP)	AI medical device evaluation (WBP)	Necrotic tissue (%) (AI medical device)
 a	D	D	7.3%
 b	D	D	37.6%
 c	D	D	96.4%

Moreover, to further analyse how all the other measurements compared with those of the AI medical device, the wounds were classified into 13 sizes, ranging from 2–2.8 cm^2 to those >33.6cm^2. Table 6 shows the mean percentage error for all of the size classes regarding all the systems used. Accuracy was derived by calculating the percentage differences of each single measurement taken with the AI medical device compared with that obtained with the other devices. As is shown in Table 6, the highest differences come through comparing the measurements obtained with MOWA. As mentioned above, this system presented less measurement ability than the rest. On the other hand, the comparison of the measurements performed with Silhouette and VISITRAK presents lower differences. The highest were obtained measuring wounds of 2–2.8cm^2 (with a 10% and a 15% difference, respectively). In these particular cases, the results were accepted since an absolute difference would be 0.28cm^2

© 2020 MA Healthcare ltd

Downloaded from magonlinelibrary.com by 130.192.232.213 on December 16, 2020.

Fig 8. Box plots of population distributions of the area measurements. Box plots showing the outliers (**a**); and box plots with the outliers removed from the analysis (**b**). WV—Wound Viewer

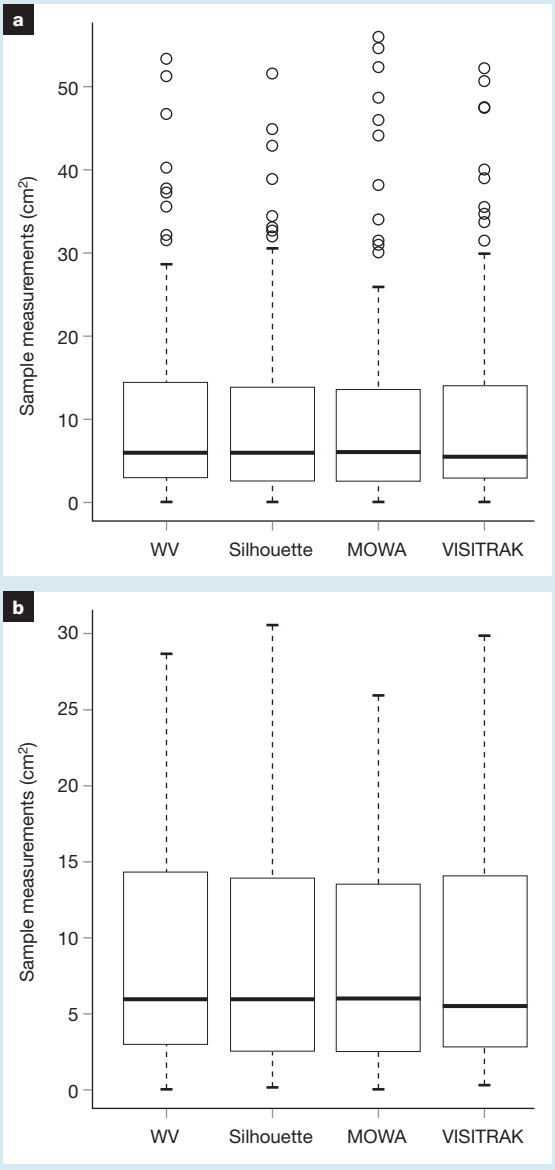
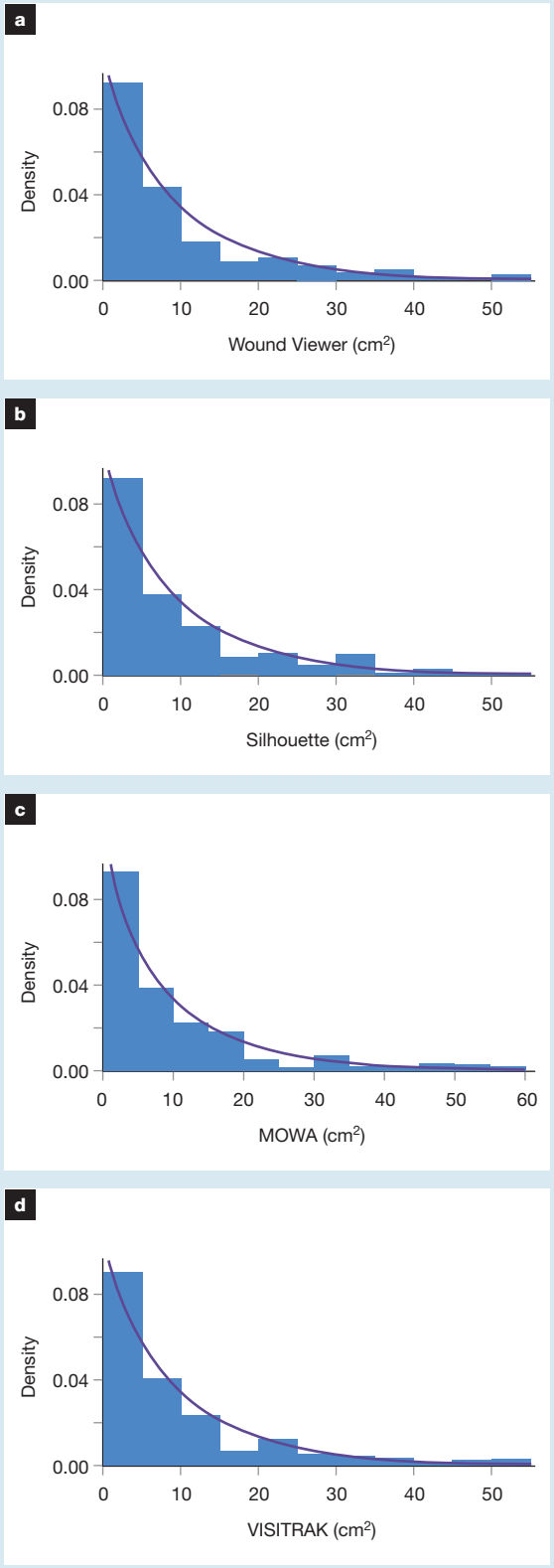


Fig 9. Population distributions of area measurements. The representations are overlapped on a kernel demonstrating how the populations present a Weibull distribution. Population measured with Wound Viewer (**a**), with Silhouette (**b**), with MOWA (**c**) and with VISITRAK (**d**)



at the most for Silhouette and 0.42cm^2 for VISITRAK, which are both clinically irrelevant.

The final analysis addresses the problem of assessing the accuracy of the depth measurements of wounds. This study compared the data obtained from Wound Viewer with the corresponding measurements collected either manually with cotton buds by the physician or using Silhouette. An initial graphical descriptive analysis in Fig 11 shows how the three populations have quite similar mean values, suggesting that the three measuring methods are consistent with each other.

However, as shown in the histograms of Fig 12, the data collected manually are distributed less consistently

© 2020 MA Healthcare ltd

Downloaded from magonlinelibrary.com by 130.192.232.213 on December 16, 2020.

Fig 10. Scatter plot of the wound area measurements taken with the AI medical device compared with the other devices (**a**). Residuals of the regression regarding the comparison of the area measurements obtained with Wound Viewer and Silhouette (**b**); Wound Viewer and MOWA (**c**); Wound Viewer and VISITRAK (**c**)

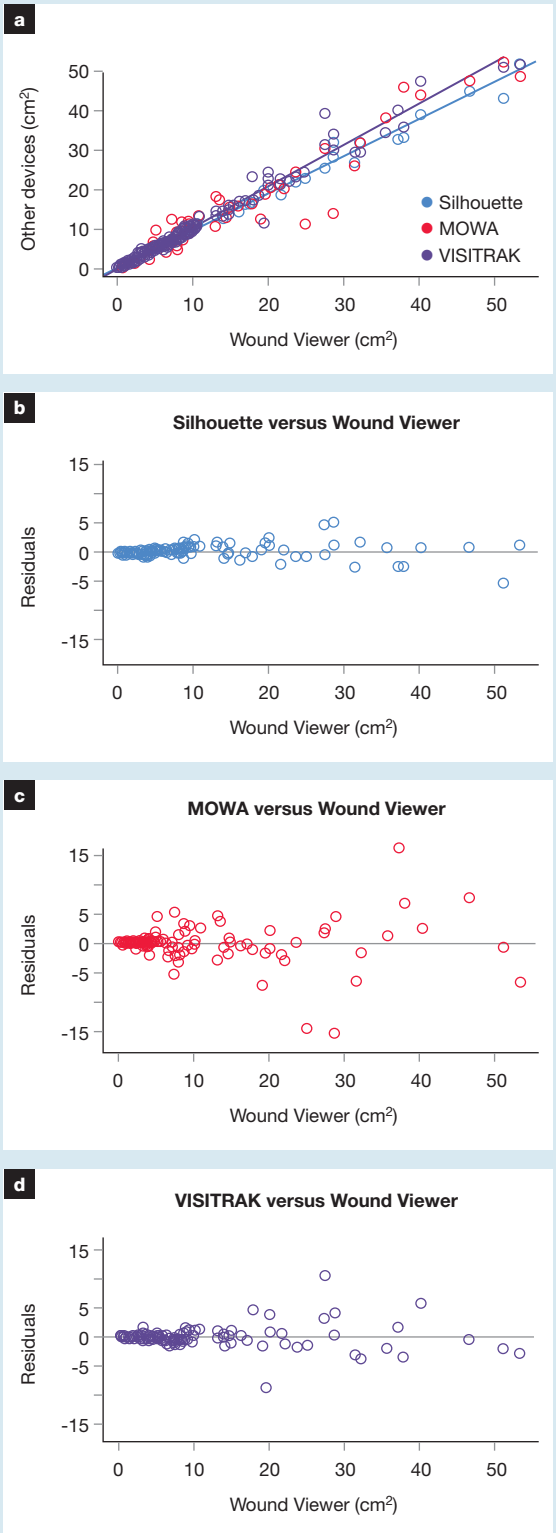
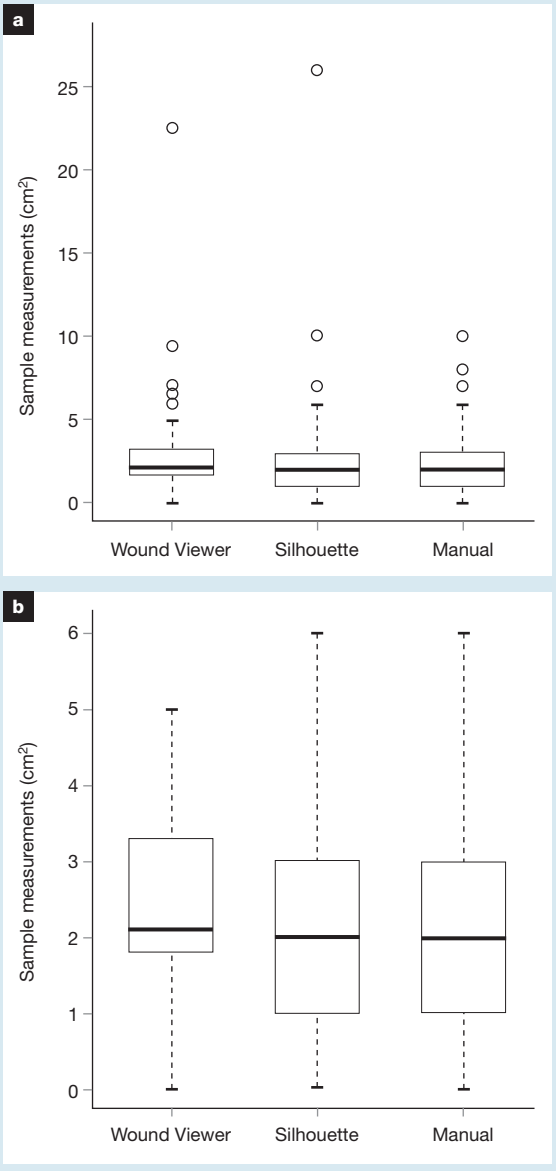


Fig 11. Box plots of the population distributions regarding depth measurements. Box plots showing the outliers (**a**) and with the outliers removed from the analysis (**b**)



than those collected by Wound Viewer and Silhouette. This may be due to inaccurate measurements using cotton buds or, in extreme cases in which a patient is in so much pain, where data collection becomes impossible.

Due to the irregular distribution of the manual measurements, it became necessary to focus only on the similarities between the data collected by the two devices. Performing a Kruskal–Wallis one-way ANOVA, the test resulted in a p-value of 0.3, attesting that there was insufficient evidence to accept the hypothesis that there are no differences between the two distributions. This is also confirmed in the scatter plots of Fig 13,

© 2020 MA Healthcare ltd

Downloaded from magonlinelibrary.com by 130.192.232.213 on December 16, 2020.

Table 6. Mean percentage measurement error regarding wound areas

	Mean percentage area measurement error												
Range (cm^2)	**0–2.8**	**2.8–5.6**	**5.6–8.4**	**8.4–11.2**	**11.2–14**	**14–16.8**	**16.8–19.6**	**19.6–22.4**	**22.4–25.2**	**25.2–28**	**28–30.8**	**30.8–33.6**	**>33.6**
Silhouette	0.1	0.05	0.05	0.03	0.05	0.04	0.1	0.03	0	0.06	0.06	0.07	0
MOWA	0.3	0.18	0.1	0.14	0.29	0.48	0.12	0.04	0.06	0	0	0.06	0.11
VISITRAK	0.15	0.09	0.07	0.06	0.28	0.04	0.03	0.04	0.09	0	0.03	0.03	0.06

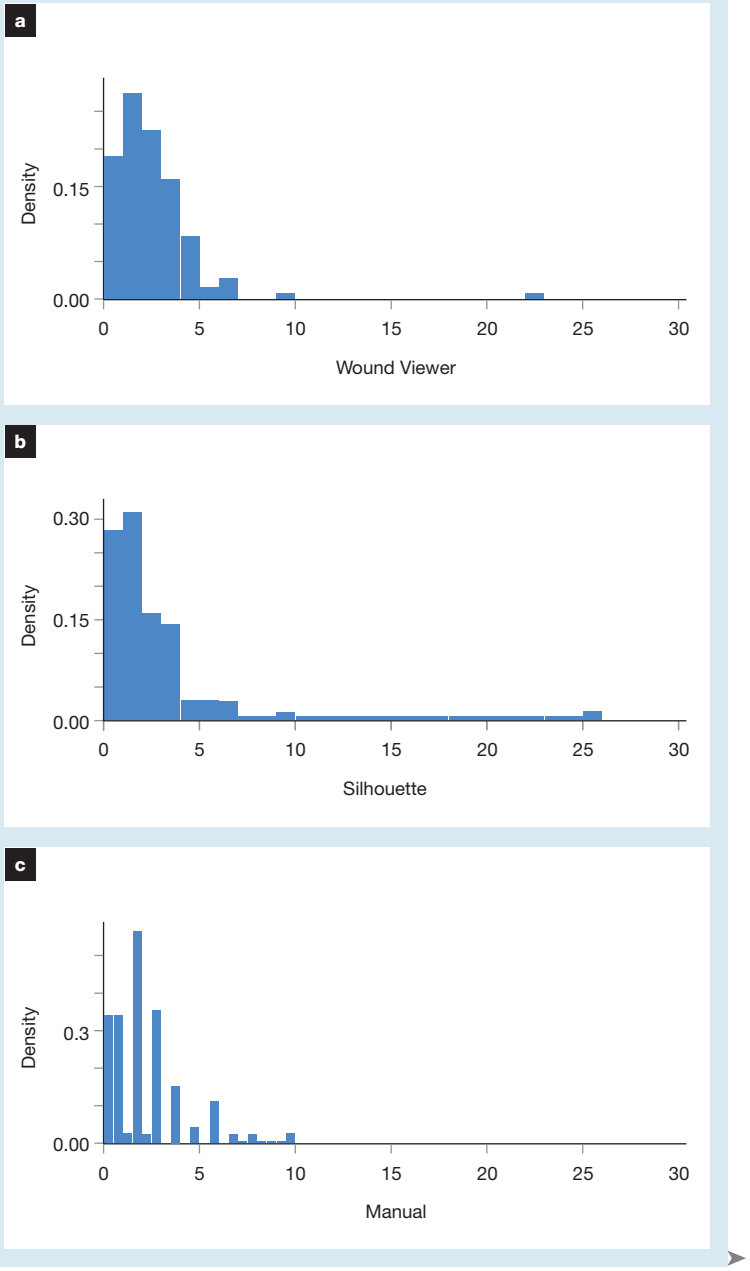
which show a distribution of points along the diagonal and residuals distributed around the horizontal axis. Taking into account shallow wounds (up to 2.8cm^2), and using Silhouette as an imperfect control, the mean relative error between the measurements of the two devices was around 10%. On the contrary, in deeper wounds the error margin ranged from 2–6%, maintaining the clinical relevance for the measurement.

Discussion

The study aimed to assess the telemedical functions and fully automated assessment capabilities of the innovative AI medical device technology through a comparative clinical trial. The AI medical device was designed and developed as a comprehensive and automatic tool using standardised data acquisition methodology to identify minimal variations in wounds from both a clinical and morphological point of view. Moreover, the telemedical capabilities of the device were tested to ensure the clinical completeness, precision and reliability of the collected data. The AI medical device assessment also looked at how easily health professionals involved in the patients' care could access and share data. This state-of-the-art development in clinical research underlines that the correct evaluation of wound bed composition and correct measurement of the wound are two vital points in rapid and efficient healing management.

The AI medical devices uses an artificial intelligence algorithm that has been trained to identify these parameters through an effective analysis of images as well as all wound characteristics regarding the tissue, so it can act like an experienced physician. The WBP score has allowed us to reach our goals regarding wound classification; Falanga put this classification forward to give physicians a better and faster understanding of wound conditions to enable more prompt intervention.[11,32] It must be noted that, in standard clinical practice, the identification of eschar is of vital importance, especially at an early stage, in order to avoid major clinical complications. Following the WBP score, with eschar present at any level of granulation, a wound is classified as 'D'. The AI medical device was able to correctly classify the wounds according to their tissue. Moreover, regarding the presence of eschar, the device was able to identify even very small amounts, as shown in Fig 5, 6 and 7, in properly classifying all critical wounds as 'D'.

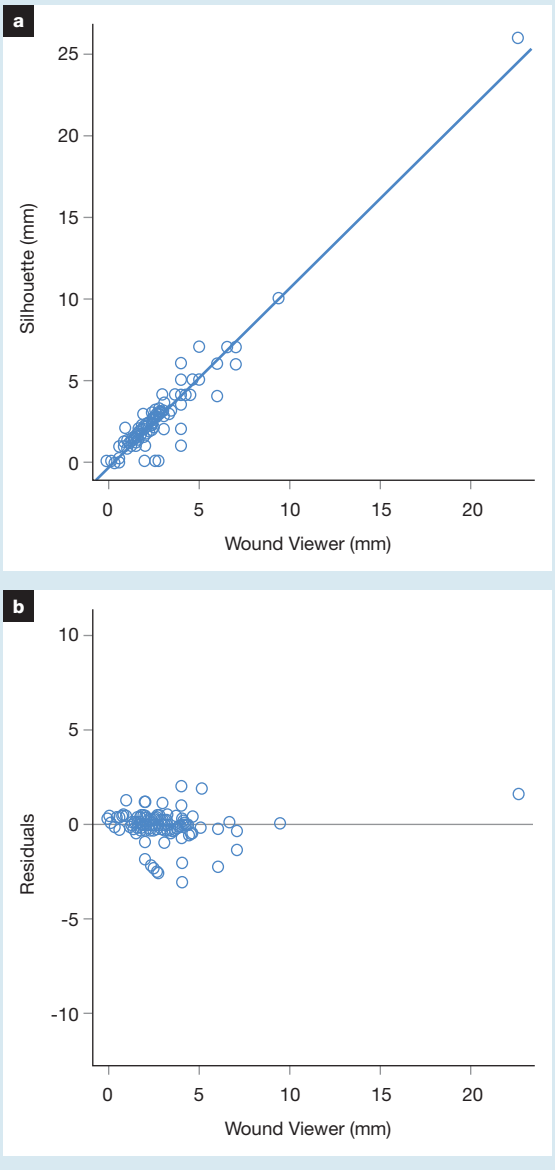
Fig 12. Histograms of population distributions regarding depth measurements. Distribution representing the measurements obtained through Wound Viewer (**a**), through Silhouette (**b**) and with a scaled probe (manual measurement) (**c**)



© 2020 MA Healthcare ltd

Downloaded from magonlinelibrary.com by 130.192.232.213 on December 16, 2020.

Fig 13. Scatter plot of the depth measurements taken with Wound Viewer compared with those obtained with Silhouette (**a**). Residuals of the regression regarding the comparison of the depth measurements obtained with Wound Viewer and Silhouette (**b**)



Limitations

The reported study was designed to include a cohort of patients presenting with a range of wounds considered to be the most comprehensive. As reported in the study design and protocol section of this paper, patients were subdivided in three main groups according to the typology of the wound. The group that reported lower limb wounds was composed of patients affected by wounds of different aetiologies that ranged from venous ulcers (approximately 40% of the cases), arterial ulcers (approximately 20% of the cases) and ulcers of other nature (the remaining approximately 40%). This particular group of patients does not represent the entire range of possible aetiologies. The results of the trial state that the AI medical device system is able to perform correct measurements and assessments on the population that was enrolled for the study. Further work and studies are under development in order to perform a set of different trials directly aimed at particular wound aetiologies to assess the actual clinical benefit that derives from telemedical precise wound assessment in different wound classes with patients who will receive a periodical follow-up.

In addition, as reported in Table 2, patients presenting wounds with presence of undermining were not included in the trial due to technical limitations of the device. Further developments are ongoing in order to render the system able to detect these conditions.

Conclusion

In this study, the AI medical device proved to be a valid monitoring tool for the prevention of dermatological complications. Its capability to acquire and store precise information of the clinical evolution of lesions permits health professionals to promptly act with appropriate therapy based on the characteristics of the wound and the patient.

Furthermore, other methods used in clinical practice for the morphological measurement of the wounds were also compared. The trial demonstrated, with statistical evidence, that the measurements performed by the AI medical device are reliable and precise, and less invasive than some other methods. This trial is the first to test and demonstrate that the AI medical device meets the criteria for which it was designed: constituting a complete, standardised and non-invasive method for classifying dermatological lesions and monitoring their clinical evolution over a clinician-specified time.

Telemedicine is at the forefront of integrative technology with the goal of improving clinical care while reducing costs in all medical fields, from mental health to nutrition. The AI medical device was designed to address an urgent clinical need within dermatology and abide by the necessary standards of quality and privacy. The classification and measurement capabilities of the AI medical device and the possibility to transmit this data makes the device an efficient telemedical tool for the remote monitoring of hard-to-heal wounds, meeting the standards necessary to be socially and clinically effective. Using the device, non-physicians can acquire remote data without compromising quality or clinical standards, enabling physicians to treat and monitor remote wound data efficiently. **JWC**

Acknowledgements: The authors would like to thank everyone who contributed both clinical and engineering knowledge to this project, such as Professor Emilio Paolucci and the TTO office of Politecnico di Torino. The authors would like to thank the following institutions for their support: Politecnico di Torino, Clinica San Luca and Incubatore Imprese Innovative of Politecnico di Torino (I3P).

© 2020 MA Healthcare ltd

Downloaded from magonlinelibrary.com by 130.192.232.213 on December 16, 2020.

Reflective questions

- Is objective wound measurement and assessment a key factor for faster wound healing?
- Will a structured telemedical system, well implemented in the standard hospital's home care procedures, render the best quality of care and promptness of intervention possible?
- Is artificial intelligence the new instrument for caregivers, able to perform an in-depth wound assessment and provide ready-to-use information in order to identify the most critical cases?

References

1 Nussbaum SR, Carter MJ, Fife CE et al. An economic evaluation of the impact, cost, and Medicare policy implications of chronic nonhealing wounds. Value Health 2018; 21(1), 27–32. https://doi.org/10.1016/j.jval.2017.07.007

2 Graves N, Zheng H. The prevalence and incidence of chronic wounds: a literature review. Wound Practice & Research. Journal of the Australian Wound Management Association 2014; 22(1):4

3 Sheehan P, Jones P, Caselli A et al. Percent change in wound area of diabetic foot ulcers over a 4-week period is a robust predictor of complete healing in a 12-week prospective trial. Diabetes Care 2003; 26(6):1879–1882. https://doi.org/10.2337/diacare.26.6.1879

4 Ferreira MC, Tuma Júnior P, Carvalho VF, Kamamoto F. Complex wounds. Clinics (São Paulo) 2006; 61(6):571–578. https://doi.org/10.1590/S1807-59322006000600014

5 Hersh WR, Hickam DH, Severance SM et al. Diagnosis, access and outcomes: update of a systematic review of telemedicine services. J Telemed Telecare 2006; 12(2_Suppl):S3–S31. https://doi.org/10.1258/135763306778393117

6 Khoo R, Jansen S. The evolving field of wound measurement techniques: a literature review. Wounds 2016; 28(6):175–181

7 Haghpanah S, Bogie K, Wang X et al. Reliability of electronic versus manual wound measurement techniques. Arch Phys Med Rehabil 2006; 87(10):1396–1402

8 Pillon S; for the European Public Health Alliance. Telemedicine and wound care management service in the Italian public healthcare system: lessons learned. 2019. https://epha.org/telemedicine-and-wound-care-management-service-in-the-italian-public-healthcare-system-lessons-learned (accessed 10 November 2020)

9 Smith-Strøm H, Igland J, Østbye T et al. The effect of telemedicine follow-up care on diabetes-related foot ulcers: a cluster-randomized controlled noninferiority trial. Diabetes Care 2018; 41(1):96–103. https://doi.org/10.2337/dc17-1025

10 Bolton L. Telemedicine improves chronic ulcer outcomes. Wounds 2019; 31(4):114–116

11 Falanga V. Classifications for wound bed preparation and stimulation of chronic wounds. Wound Repair Regen 2000; 8(5):347–352. https://doi.org/10.1111/j.1524-475X.2000.00347.x

12 Mani R, Falanga V, Shearman C, Sandeman D. Clinical aspects of lower limb ulceration in chronic wound healing. London: WB Saunders; 2009

13 Gethin, G. The significance of surface pH in chronic wounds. Wounds UK 2007; 3(3):52

14 Flanagan M. Wound measurement: can it help us to monitor progression to healing? J Wound Care 2003; 12(5):189–194. https://doi.org/10.12968/jowc.2003.12.5.26493

15 Sheehan P, Jones P, Caselli A et al. Percent change in wound area of diabetic foot ulcers over a 4-week period is a robust predictor of complete healing in a 12-week prospective trial. Diabetes Care 2003; 26(6):1879–1882. https://doi.org/10.2337/diacare.26.6.1879

16 Gorin DR, Cordts PR, LaMorte WW, Menzoian JO. The influence of wound geometry on the measurement of wound healing rates in clinical trials. J Vasc Surg 1996; 23(3):524–528. https://doi.org/10.1016/S0741-5214(96)80021-8

17 Cukjati D, Reberšek S, Miklavcic D. A reliable method of determining wound healing rate. Med Biol Eng Comput 2001; 39(2):263–271. https://doi.org/10.1007/BF02344811

18 Falanga V, Saap LJ, Ozonoff A. Wound bed score and its correlation with healing of chronic wounds. Dermatol Ther 2006; 19(6):383–390. https://doi.org/10.1111/j.1529-8019.2006.00096.x

19 Grey JE, Enoch S, Harding KG. Wound assessment. BMJ 2006; 332(7536):285–288. https://doi.org/10.1136/bmj.332.7536.285

20 Tong A. The identification and treatment of slough. J Wound Care 1999; 8(7):338–339. https://doi.org/10.12968/jowc.1999.8.7.25895

21 Thomas AM, Harding KG, Moore K. The structure and composition of chronic wound eschar. J Wound Care 1999; 8(6):285–287. https://doi.org/10.12968/jowc.1999.8.6.25881

22 Durham DR, Fortney DZ, Nanney LB. Preliminary evaluation of vibriolysin, a novel proteolytic enzyme composition suitable for the debridement of burn wound eschar. J Burn Care Rehabil 1993; 14(5):544–551. https://doi.org/10.1097/00004630-199309000-00009

23 Ramundo J, Gray M. Enzymatic wound debridement. J Wound Ostomy Continence Nurs 2008; 35(3):273–280. https://doi.org/10.1097/01.WON.0000319125.21854.78

24 Farina M, Secco J. Live demonstration: 3D wound detection & tracking system based on artificial intelligence algorithm. IEEE Biomedical Circuits and Systems Conference (BioCAS) Turin 2017; 1. https://doi.org/10.1109/BIOCAS.2017.8325105

25 Itoh M, Chua L. Memristor cellular automata and memristor discrete-time cellular neural networks. Int J Bifurcat Chaos 2009; 19(11):3605–3656. https://doi.org/10.1142/S0218127409025031

26 Secco J, Farina M, Demarchi D et al. Memristor cellular automata for image pattern recognition and clinical applications. IEEE International Symposium on Circuits and Systems (ISCAS) Montreal 2016: 1378–1381. https://doi.org/10.1109/ISCAS.2016.7527506

27 Secco J, Farina M, Demarchi D, Corinto F. Memristor cellular automata through belief propagation inspired algorithm. International SoC Design Conference (ISOCC) Gyungju 2015: 211–212. https://doi.org/10.1109/ISOCC.2015.7401793

28 Secco J, Poggio M, Corinto F. Supervised neural networks with memristor binary synapses. Int J Circuit Theory Appl 2018; 46(1):221–233. https://doi.org/10.1002/cta.2429

29 Chua L. Memristor–the missing circuit element. IEEE Trans Circuit Theory 1971; 18(5):507–519. https://doi.org/10.1109/TCT.1971.1083337

30 Chua LO, Yang L, Krieg KR. Signal processing using cellular neural networks. In: Nossek JA (ed). Parallel processing on VLSI arrays. Springer; 1991

31 Chua LO, Yang L. Cellular neural networks: theory. IEEE Trans Circ Syst 1988; 35(10):1257–1272. https://doi.org/10.1109/31.7600

32 Schultz GS, Barillo DJ, Mozingo DW, Chin GA; Wound Bed Advisory Board Members. Wound bed preparation and a brief history of TIME. Int Wound J 2004; 1(1):19–32. https://doi.org/10.1111/j.1742-481x.2004.00008.x



© 2020 MA Healthcare ltd

Downloaded from magonlinelibrary.com by 130.192.232.213 on December 16, 2020.